Rasayely
Membrane Science International
https://rasayely-journals.com/index.php/msi
Vol 1(2); 44–53 2022

Original Article Open Access

Preparation and Performance Control of Orcinol Composite Nanofiltration Membrane for Dimethyl Sulfoxide Recovery

Ayang Zhou[1,*], Mengying Li[1], Lin Li[1], and Yujie Wang[1]

[1]*College of Materials and Chemical Engineering, Chuzhou University, Chuzhou 239000, China*

[*]Author to whom any correspondence should be addressed; e-mail: zhouayang@foxmail.com, Tel.: +86-0550-3511052. Fax: +0550-3511046

Received: 12 May 2022; Revised: 30 June 2022; Accepted: 14 July 2022; Published: 01 September 2022

Academic Editor: Wilfredo Yave, Research and Development Department, DeltaMem AG, Switzerland

Abstract

As a new separation technology, organic solvent nanofiltration (OSN) membrane technology has been increasingly applied in the separation of small molecular compounds in various organic solvents due to its energy saving and high efficiency. Dimethyl sulfoxide (DMSO) is an important solvent in pharmaceutical and catalytic industries, and its recovery has attracted more and more attention. An OSN membrane is firstly constructed by orcinol (OL) and trimesoyl chloride (TMC) via interfacial polymerization (IP). The prepared OSN membrane achieves a crystal violet (CV, 407.99 g/mol) rejection of higher than 92% and a DMSO permeance of 3.0 L m^{-2} h^{-1} bar^{-1}. The chemical characterization methods such as X-ray photoelectron spectroscopy and attenuated total reflectance Fourier transform infrared spectroscopy are used to indicate that the composite membrane is composed of a polyarylester top layer. To enhance the permeance while maintaining its superior rejection toward CV in DMSO, urea is used as a modifier during IP process. As consequence, the hydrophobicity of the membrane surface is improved, the contact angle increases from 62° to 85°, and the modified poly(amide-co-ester) structure on the top layer is formed. The permeance of urea modified membrane reaches 4.7 L m^{-2} h^{-1} bar^{-1}. The long-term OSN filtration shows that the membrane has a DMSO permeance of 4.6 L m^{-2} h^{-1} bar^{-1}, with CV rejections over 90%. The architecture of the poly(amide-co-ester) top-layer provides a new route for the fabrication of OSN membranes.

Keywords:

Orcinol; solvent resistance; dimethyl sulfoxide; trimesoyl chloride; interfacial polymerization; urea

1. Introduction

As an important chemical raw material, dimethyl sulfoxide is widely used in chloroaniline, acrylic acid, aromatic extraction, esterification accelerator, capacitor, paint remover, wax refining, pesticide synergist, etc. Membrane separation technology can be used for dimethyl sulfoxide recovery, which is better than distillation in terms of investment, energy consumption and environmental protection, extraction, and other traditional methods [1–3]. Solvent-resistant nanofiltration membrane technology can be used for separating small molecular compounds in organic solvents, which is a green technology to solve energy-saving and environmental problems and to the national development strategy. The biggest challenge facing its preparation technology is to achieve effective regulation of the functional top-layer of the composite membrane during the preparation process [4–10].

Interfacial polymerization technology is the main method to prepare OSN membrane at present. For instance, Gohain *et al.* synthesized a membrane using piperazine aqueous monomer solution incorporating a composite of a mixture of hectorite and UiO-66-NH_2 reacted with TMC. The prepared TFN membrane showed a permeance of 80.68 L/m^2.h in humic acid [11]. Polyamide solvent-resistant composite membrane is currently the most developed solvent-resistant composite membrane by IP method. He *et al.* synthesized

an OSN membrane using the mixture of ethylenediamine and p-xylylenediamine and 1,2,4,5-benzene tetracarbonyl chloride as reactive monomers, the membrane shows a permeance of 0.6.1 L $m^{-2}h^{-1}$ bar^{-1}in DMF [12]. Almijbilee *et al.* used 4,4′-oxydianiline to react with TMC to fabricate an OSN membrane. The prepared membrane showed a THF permeance of 0.45 L m^{-2} h^{-1} bar^{-1} [4]. Recently, preparing solvent-resistant polyester composite membrane has gradually become one of the research hotspots [13,14]. Solomon *et al.* used contorted phenols TTSBI reacted with TMC by IP reaction, and the membrane showed a permeance of 4.01 L m^{-2} h^{-1} bar^{-1} in THF [15]. Abdellah *et al.* prepared a polyester membrane using catechin and terephthaloyl chloride as reactive monomers, the prepared membrane exhibited a permeance of 1.2 L m^{-2} h^{-1} bar^{-1} in DMF [16].

A novel trend is the development of ultrathin free-standing membranes with rigidly intrinsic pores for rapid and precise molecular separation. Zhu *et al.* regulated the thickness of the membrane from 32.3 to 5.6 nm by using glycerol as an additive [17]. Zhai *et al.* constructed a polyarylate film from Noria, a porous organic cage, and terephthaloyl chloride (TPC) through interfacial polymerization. the Noria-TPC membrane showed a permeance of 18 L m^{-2} h^{-1} bar^{-1} in methanol [18].

Bio-nanocomposite polymer materials and membranes have attracted much attention [19,20]. Lignin and its derivatives, such as vanilla alcohol and vanillin, are natural polymers, which are reported to exhibit low solubility in organic solvents [21–23]. In our previous research, lignin and its model compounds have strong solvent resistance as aqueous monomers. These compounds have highly reactive phenolic hydroxyl groups to prepare solvent-resistant composite membrane [24–26].

To find more monomers similar to lignin to prepare OSN membranes, orcinol was selected and carried out interface polymerization with TMC in the previous study [27]. The results show that microwave heating can reduce the pore size of the membrane and increase the rejection of the membrane. The optimal membrane exhibited a rejection of 98% for crystal violet (CV) but a low permeance of 1.8 L m^{-2} h^{-1} bar^{-1} [27]. To prepare an orcinol solvent-resistant composite nanofiltration with high permeance and high rejection from the perspective of top-layer property regulation. This work focused on changing the hydrophobicity of the membrane surface to improve the DMSO permeance of OSN membranes. Herein, urea is selected as a modifier to improve the hydrophobicity of the OL-TMC membrane and form a stable polyureamide structure to avoid the tradeoff effect and reduce membrane rejection. The results imply the simple modification method to increase the permeance of the membrane, which has a great superiority for the commercialization of the OSN membrane. This work proposed an effective post-synthetic modification method to improve the permeance of OSN membranes in polar aprotic solvent without reducing rejection, which might give guidance to the fabrication of optimized high-performance OSN membranes.

2. Experimental

2.1. Experimental Raw Materials

Ultem 1000 (Polyetherimide, PEI) was purchased from SABIC (Saudi Arabia). Orcinol (CAS: 504-15-4) was supplied by Lanji (Shanghai, China). Trimesoyl chloride (CAS: 4422-95-1) was purchased from Heowns (Tianjin, China). Polypropylene non-woven was supplied by Teda (Tianjin, China). Dimethylacetamide (DMAc), Ethylenediamine, Dimethyl sulfoxide (DMSO), and Tetrahydrofuran (THF) were purchased from Kemiou (Tianjin, China). 4-Dimethylaminopyridine was supplied by Macklin (China) as a phase transfer catalyst for interfacial polymerization. All reagents were not purified further.

2.2. Preparation of Nanofiltration Membrane

The preparation method of polyetherimide (PEI) support is as follows: dissolve 23% polyetherimide solution in DMAC in a three-neck flask with a stirring rod, the stirring temperature is 60 °C, the stirring time is 4 hours, and the stirring speed is 500 (rad/min). Then, scrape the DMAc-PEI solution evenly on non-woven fabric, and keep the distance at 150 μm. The membrane is then placed in 25 °C water for phase transfer and removed after 1 hour. Then, the PEI membrane is put into a 6% ethylenediamine methanol solution (w / V) for 1 hour to improve the solvent resistance. The preparation process of the orcinol composite membrane is carried out in a 25°C incubator. The crosslinked membrane is immobilized on a Teflon frame. First, a certain concentration of orcinol solution mixed with 0.5% (w / V) DMAP, is poured onto the surface of the crosslinked membrane and stood for 2 minutes. The mixture of TMC and hexane mixture 0.1 (w / V) is poured onto the surface of the membrane and the reaction time is set to 1 minute. Then the membrane is put into an oven at 70 ° C for 6 minutes of heat treatment. As shown in **Figure 1**, the preparation of urea modified membrane is as follows. After the interfacial polymerization reaction of orcinol and TMC for 1 minute, 100 ml of ethanol solution of urea was poured onto the top layer, and the prepared membrane is named NF-XOL-YU, where X represents the concentration of orcinol and Y represents the mass of urea (g). One membrane was named NF-C, which is crosslinked by EDA and then directly injected with TMC for comparison.

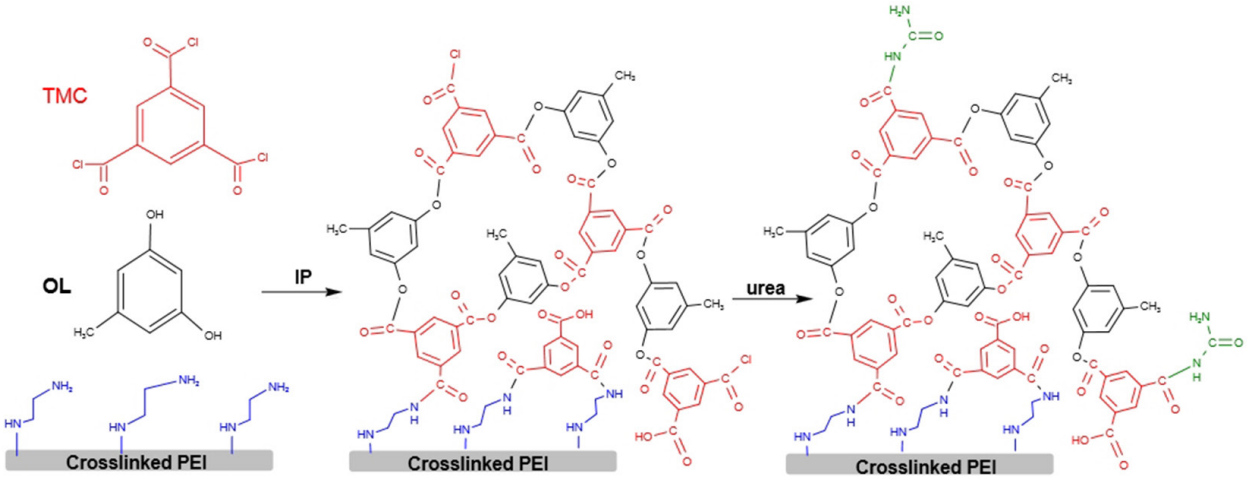

Figure 1: A possible interfacial polymerization mechanism of OL and TMC, modiflied by urea.

2.3. Characterization of the Materials

The surface and cross-section morphologies of the prepared membranes are investigated using an LEO 1550 VP (Germany) scanning electron microscope (SEM). X-ray electron spectroscopy (Thermo, USA) characterizes the chemical composition of the membrane surface. Atomic force microscopy (Seiko, Japan), characterizing the membrane surface morphology, is measured at least three times. The static contact angle measuring instrument (JC2000D1, Shanghai) is used to characterize the hydrophilicity of the membrane. Each batch of samples is measured 5-6 times and the average value is taken.

2.4. Characterization of Membrane Separation Performance

The separation adopts a separation dead-end device made of stainless steel, the effective area of the membrane is 38.5 cm^2, and the separation pressure is 1MPa.

The permeance could be calculated by Eq. **(1)**:

$$P = \frac{V}{A \times t \times \Delta P} \quad (1)$$

P—Permeance of Membrane, $L \cdot m^{-2} \cdot h^{-1} bar^{-1}$;
V—The fractionated filter volume, L;
A—Separation area, m^2;
T—Effective separation time, h;
ΔP—Trans-membrane pressure difference, bar.

The rejection rate can be calculated according to the concentration of mother liquor and penetrating liquor, which can be calculated by Eq. **(2)**:

$$R = \left(1 - \frac{C_p}{C_f}\right) \times 100 \quad (2)$$

R—Rejection rate, %;
C_p—Concentration of solute in the permeate fraction, $g \cdot L^{-1}$;
C_f—Concentration of raw material liquid, $g \cdot L^{-1}$.

Swelling experiments in organic solvents are used to test the stability of the membranes After being weighed, dry membranes were soaked in the solvent for 7 days. Then membranes were wiped dry with filter paper. The swelling was calculated as Eq. **(3)**:

$$S = \frac{\left(\frac{m_{eq} - m_d}{m_d}\right)}{\rho_s} \quad (3)$$

Where S, m_{eq}, m_d, and ρ_s represent the permeated swelling degree, the weight of several swollen membranes and dry membranes, and the solvent density, respectively.

3. Results and Discussion

3.1. Analysis of the Surface Chemical Properties

Figure 2 displays the ATR-FTIR characteristic spectra of the membranes including NF-C, NF-1OL, and NF-2OL. The spectra of NF-C are located at 1540 cm^{-1},1640 cm^{-1}(amide), 1793 cm^{-1} (imide group), and 3343 cm^{-1} (amine group), which are the characteristic peaks of polyamide **[28]**. Compared with NF-C, the peaks of NF-1OLand NF-2OL at 1050cm^{-1} and 1230cm^{-1} gradually increase (ester group). According to literature reports, the absorption intensity of peaks can be calculated **[25]**. In contrast, the strength of I_{1230}/I_{1643} increase and NF-2OL (0.35) > NF-1OL (0.14). It is illustrated that the monomers TMC and OL can occur IP reaction to generate the ester groups, and the structure of poly(amide-co-ester) membrane consists of more fractions of ester groups as the orcinol concentration increases.

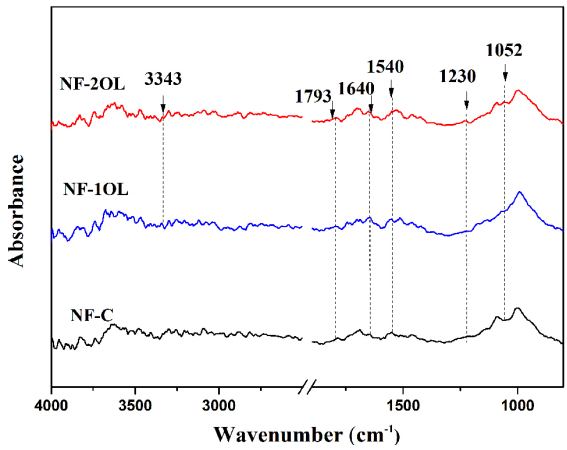

Figure 2: ATR-FTIR characteristic spectra of the membranes including NF-C, NF-1OL, and NF-2OL.

Figure 3 displays the XPS peak spectra of carbon, nitrogen, and oxygen of the NF-1OL membrane: the carbon characteristic peaks are at 285.9 ev (-C-N) 284.9 ev (-C-O), and 284.3 ev (-C-C-), respectively. The nitrogen characteristic peaks are at 400.9 ev (-N-H), 399.9 ev (-N-C = O), and 399.2 ev (-N-C), respectively. The oxygen characteristic peaks are at 533.5 eV (-O=C-O *), 532.3 ev (- OH), 531.5 ev (-C = O), and 530.7 ev (-ph-O-), respectively **[26,29]**.

3.2. Separation Properties of the Membrane

Figure 4 displays the performance of the membrane prepared from different OL concentrations while keeping the TMC concentration unchanged in the separation of DMSO solution containing dye CV. NF-C exhibits the permeance of 0.11 m^{-2} h^{-1} bar^{-1} and CV rejection of 50%. NF-1OL achieves a CV rejection and a DMSO permeance of higher than 91% and of 3.0 L m^{-2} h^{-1} bar^{-1}, respectively. When the OL concentration increases to 3g (w/V), the rejection reaches 92%. Then, the permeance of the NF-3OL decreased by 2.65 L m^{-2} h^{-1} bar^{-1}. The top layer of NF-C is composed of polyamide formed by the reaction of TMC with the terminal amino group of EDA and a thick polyamide top layer is formed on the surface of the membrane and inside the pores of the membrane. Therefore, NF-C has a low rejection rate and low permeability. For the membrane prepared with OL, the rejection increases with the increase of the concentration of OL. During the presence of OL, the IP process occurs among TMC and OL on the crosslinked PEI surfaces. The concentration of OL monomer on the surfaces is the key limiting factor that affects the formation of the top layer, however, the possible cost of high rejection is lower flux due to the trade-off effect. With a much higher OL concentration, the top layer formed via IP becomes a little denser, consequently making the permeance lower. Besides, the study on the relationship between the membrane permeance and microwave heating post-treatment method is performed as shown in Figure S1. It's indicated that microwave heating can reduce the pore size of the membrane but the permeance of the membrane decreases greatly.

Despite the NF-1OL membranes having excellent solvent resistance, the permeance is relatively low. Therefore, urea modification was adopted as a reinforcement means to optimize the membrane structure. For a nanofiltration membrane, the transport depends on the hydrophilicity, porosity, top layer thickness, and solvent properties of the membrane. Considering the weak polarity of these solvents (such as THF and DMSO), it is expected that permeance will not be high for hydrophilic membranes **[30,31]**. Urea can form a polyamide top-layer with TMC and the amide generated can change the hydrophobicity of the membrane. To further investigate the role of urea in improving membrane performance, the contact angles of membranes were separately tested. As shown in **Figure 5**, the contact angle is 65°, and 49° for NF-C and NF-1OL respectively. With the addition of urea, the contact angle increases from 62° (NF-1OL-1U) to 85° (NF-1OL-4U). The hydrophobic surface is attributed to the formation of amide on the membrane surface, which is generated by the interfacial polymerization of urea and OL.

3.3. SEM and AFM Characterization

As can be seen from **Figure 6**, NF-C, NF-1OL, and NF-1OL-2U all have asymmetric structures with finger-like pore support layers and dense skin layers. NF-C presents the peak valley structure that polyamides usually have. Compared with the irregular shape of polyester NF-1OL surface, NF-C surface presents a more regular polyamide peak valley structure, while NF-1OL-2U presents a more different morphology than NF-1OL and NF-C.

Figure 7 displays the root mean square (RMS) values of several membranes including NF-C, NF-1OL, and NF-1OL-2U were 116.98 nm, 35.38 nm, and 11.25 nm, respectively. In the process of interfacial polymerization, the diffusion rate of an aqueous monomer towards an organic solution is faster. This rapid migration can push and reverse the ultrathin films formed by the initial polymerization, thus forming ridge and valley structures. With increasing urea, the surface of NF-1OL-2U becomes smooth and dense.

Figure 8 shows the effect of urea concentration on membrane performance. As the urea concentration increases to 2g, the permeance increases to 4.75 L m^{-2} h^{-1} bar^{-1}. As the concentration of urea continues to increase, the rejection and permeance changes are not obvious. In the presence of urea, the IP process occurs among TMC, urea monomer, and OL. The coverage of TMC on the surfaces is the key limiting factor that affects the formation of the top layer, as the concentration of urea rises further higher than 2g.

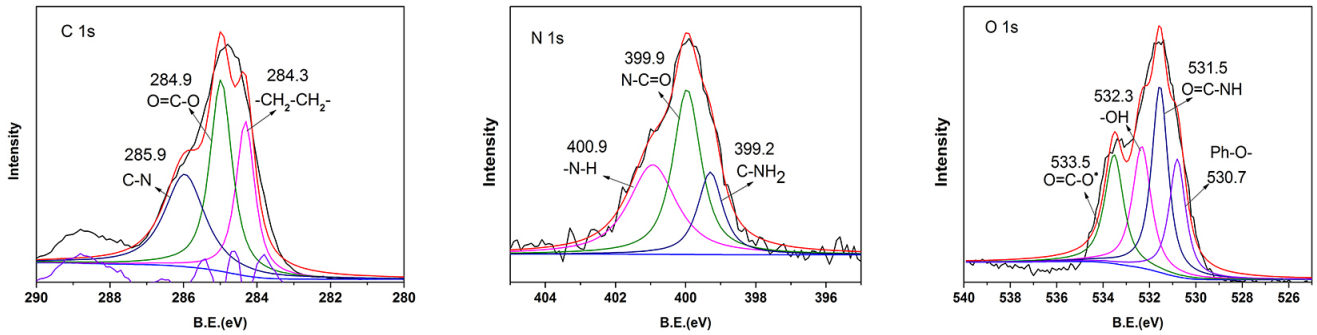

Figure 3: Deconvoluted C1s, N1s, and O1s XPS spectra for NF-1OL.

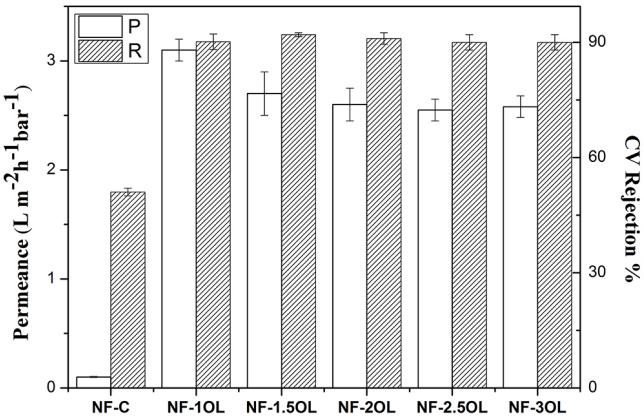

Figure 4: Performance of OL-TMC membranes with different OLconcentration (0, 5%, 1%, 1.5%, 2%,4% (w/v)) for 10 mg·L-1 CV DMSO solution at 1 MPa.

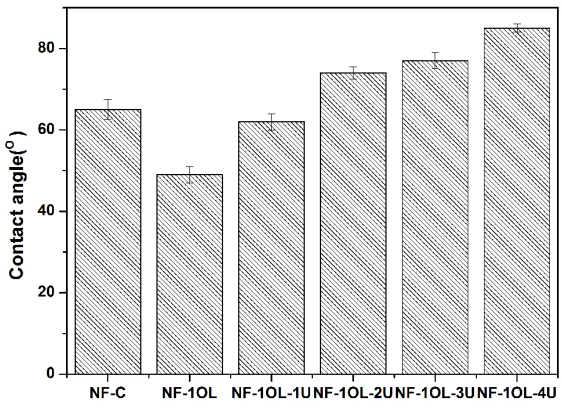

Figure 5: The static water contact angles including NF-C, NF-1OL, NF-1OL-1U, NF-1OL-2U, NF-1OL-3U, and NF-1OL-4U.

3.4. XPS Characterization

Figure 9 displays the XPS peak spectra of carbon, nitrogen, and oxygen of NF-1OL-2U. The carbon characteristic peaks at 285.9 eV (C-N) and the nitrogen characteristic peaks at 399.9 ev (N-C = O) prove the formation of polyamide. The oxygen characteristic peaks at 533.4 eV (-O=C-O *) confirm the existence of polyarylester **[32,33]**.

As shown in **Table 1**, carbon contents are 61.1%, 71.2.6% and 62.54%, nitrogen contents are 21.11%, 9.8% and 18.21%, and oxygen contents are 17.79%, 19.04% and 19.25% for NF-C, NF-1OL and NF-1OL-2U respectively. Compared with NF-C, the oxygen content of NF-1OL increases, derived from the formation of polyarylester. When adding urea, the nitrogen content of the membrane surface gradually increases and the carbon content decreases.

To further explore the effect of adding urea on interfacial polymerization, in situ UV-Vis test is also selected to observe the changes of carbonyl absorbance for TMC at 279 nm, the consumption rate of TMC in n-hexane can be obtained by analyzing the absorbance change of ultraviolet light **[17,34]**. As shown in **Figure 10**, with the progress of interfacial polymerization, the absorption peak of carbonyl first decreases due to consumption in reaction, and then the absorption of TMC gradually increases due to the formation of polyarylester. When urea is added, the changing trend of the concentration of TMC becomes relatively smooth, which may be due to the introduction of more carbonyl into the system by urea. This observation may explain why the RMS value of the modified surface by urea is smaller than that of the OL-TMC membrane.

Figure 11 shows the separation performance of NF-1OL-2U in several organic solvents. The separation performance of membranes in different solvents is very different. The permeance in DMF is 3.3l L m^{-2} h^{-1} bar^{-1} and the rejection is 94%. While the permeance in THF is 3.0 l L m^{-2} h^{-1} bar^{-1} and the rejection is only 77%. In methanol, the permeance is as high as 6 L m^{-2} h^{-1} bar^{-1} and the rejection is 40%. The effects of pore size of the membrane, solvent viscosity, and the magnitude of solvent play important roles in separation performance. As shown in Table S1, the swelling ratio of NF-1OL-2U for DMSO (0.45ml/g) is much lower than that of Methanol, which indicated high chemical stability in DMSO and also explains that the membrane showed relatively large permeance and relatively low rejection when separating CV in methanol.

Table 1: C, N, O element content of NF-C, NF-1OL, NF-1OL-2U determined by XPS.

Membranes	Element content (atom.%)				
	C	N	O	C/O	O/N
NF-C	61.1	21.11	17.79	3.43	0.84
NF-1OL	71.19	9.8	19.04	3.74	1.94
NF-1OL-2U	62.54	18.21	19.25	3.24	1.05

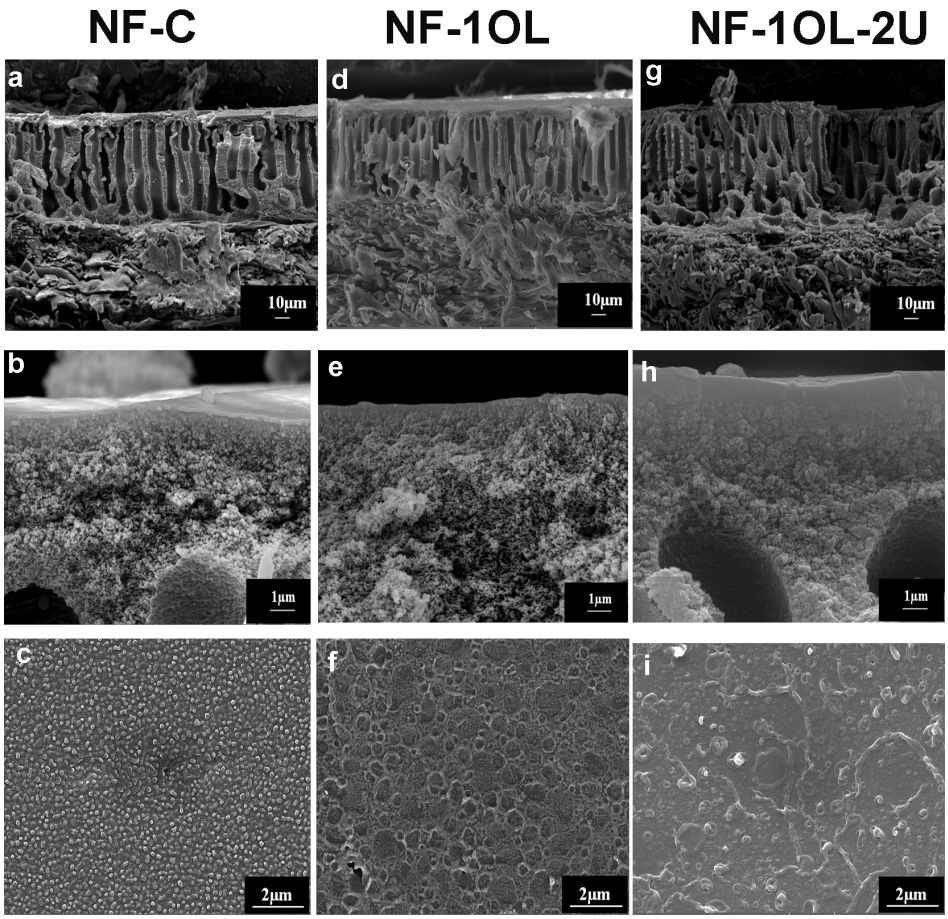

Figure 6: SEM images of the top surface and cross-sections of the TFC NF membranes including NF-C (a-c), NF-1OL (d-f), and NF-1OL-2U(g-i).

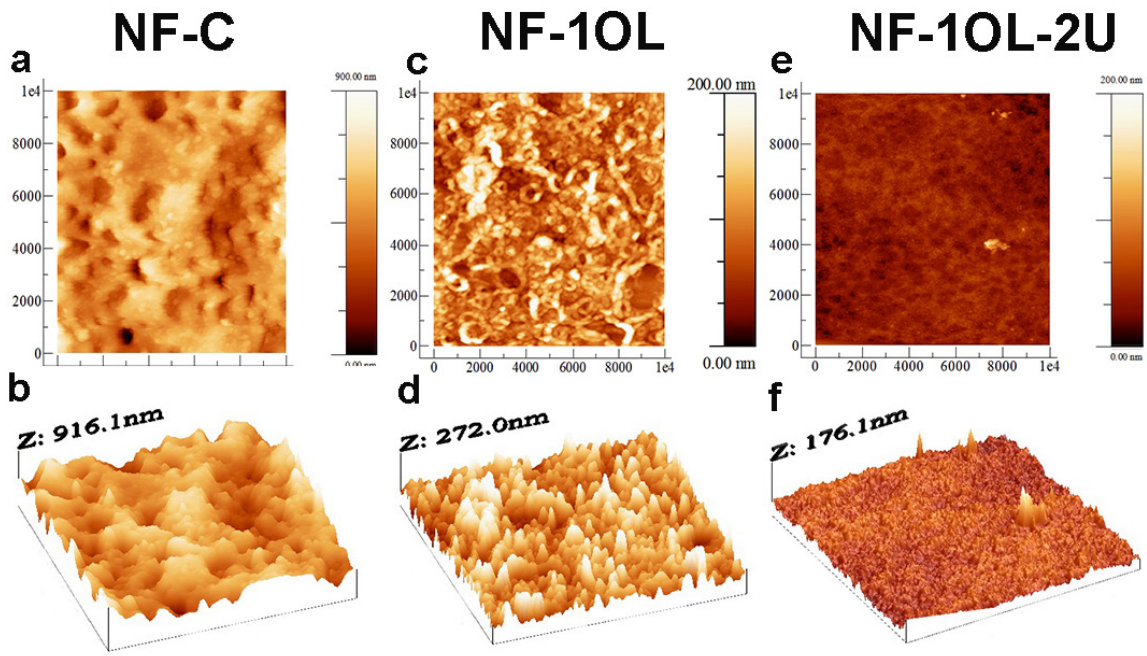

Figure 7: The Plan and 3D AFM images of several membranes including NF-C(a-b), NF-1OL (c-d), and NF-1OL-2U(e-f) membranes.

3.5. *Test of Membrane Stability*

As shown in **Figure 12**, the stability of NF-1OL-2U in DMSO was also tested in this study. The rejection remained at about 91% during 40 hours of separation. After an initial swelling caused by DMSO, the DMSO permeance decreased gradually and reached a constant value of about 4.6 L m^{-2} h^{-1} bar^{-1} which is relatively high as compared with those of other research works, as shown in **Table 2**.

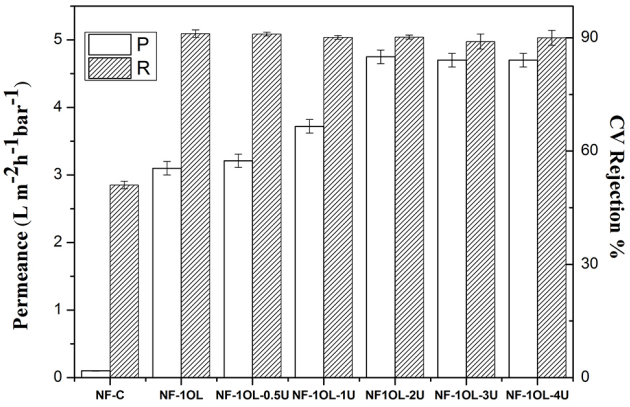

Figure 8: Performance of OL-TMC membranes with different urea concentration (0, 5%, 1 %, 2%, 3%,4% (w/v)) for 10 mg·L^{-1} CV DMSO solution at 1 MPa. (All membranes were fabricated using 0.01 % (w/v) TMC).

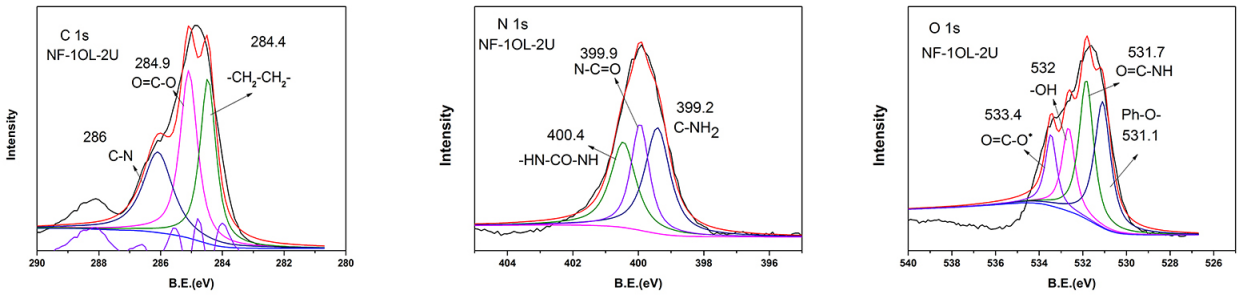

Figure 9: Deconvoluted C1s, N1s, and O1s XPS spectra for NF-1OL-2U membranes.

Table 2: Comparison of separation performance between several solvent-resistant nanofiltration membranes reported in the literature and self-made membrane materials in DMSO.

OSN Membrane	Permeance (L m^{-2} h^{-1} bar^{-1})	Solute	Molecular weight (Dalton)	Rejection (%)	Ref.
PMDA-MDA /TiO_2	6.4	RB	1017.64	89.5	[35]
Polybenzimidazole	0.31	RB	1017.64	90	[36]
PTSC-24	2.2	Direct Red	1373	>91	[37]
DAP-TMC	4.6	RB	1017.64	91	[38]
MPD-TMC	1	Tetracycline	444	>95	[39]
Electrospun PAN	1	Fast Green FCF	808	90	[40]
NF-1OL	3.1	Crystal Violet	407	91	This work
NF-1.5OL	2.6	Crystal Violet	407	92	
NF-1OL-2U	4.6	Crystal Violet	407	91	

The separation properties of some solvent-resistant composite membranes in DMSO reported in the literature were listed in **Table 2**. It can be seen from the table that the separation performance of the synthesized membranes including NF-1OL, NF-1.5OL, and NF-1OL-2U is comparable to that of the composite membranes listed.

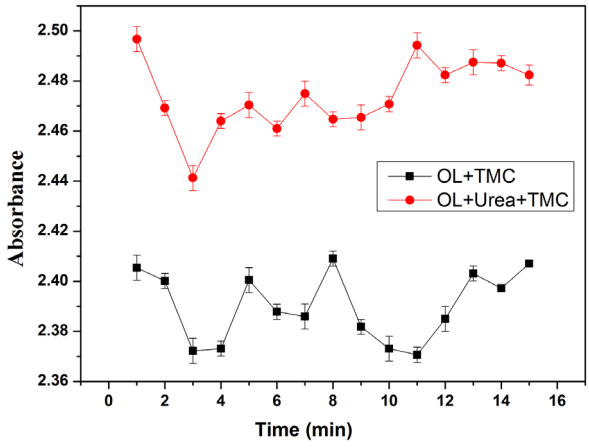

Figure 10: UV-Vis absorption of carbonyl for TMC before and after urea addition during IP reaction between OL and TMC.

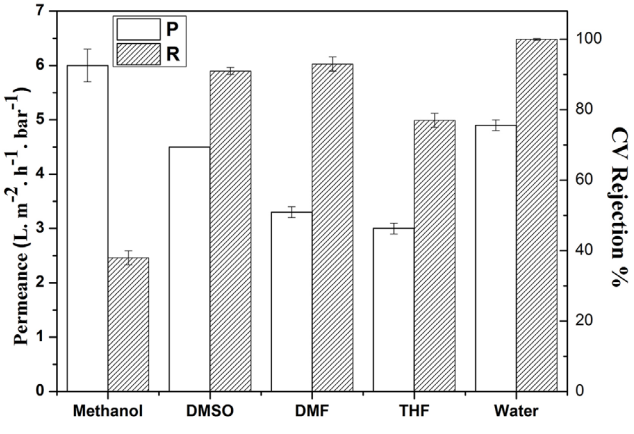

Figure 11: Separation performance of NF-1OL-2U in several organic solvents including methanol, DMSO, DMF, THF, and water.

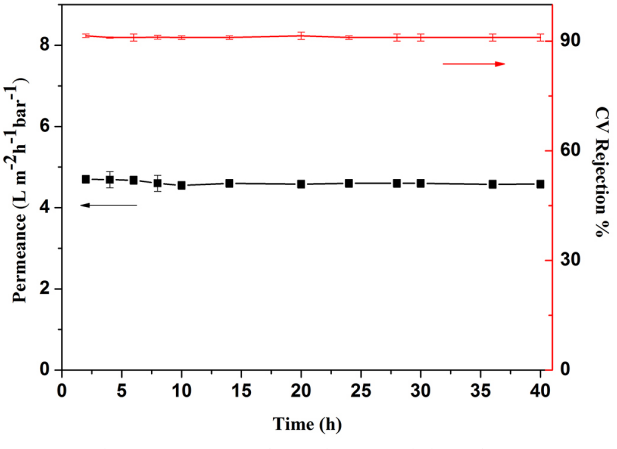

Figure 12: Characterization of membrane stability of NF-1OL-2U in DMSO for 40 hours.

4. Conclusions

Using orcinol and trimesoyl chloride as monomers, a polyarylester solvent-resistant composite nanofiltration membrane has been fabricated. The membrane with better process conditions has a rejection of 92% for CV in DMSO, and a permeance of 3.1 L m^{-2} h^{-1} bar^{-1}. Urea was used to modify the properties of solvent-resistant composite membrane for the first time, With the addition of urea, the contact angle of OL-TMC membrane increases from 62° to 85°. The membrane modified by urea shows a lower swelling ratio for DMSO (0.45ml/g) and an improved permeance of 4.6 L m^{-2} h^{-1} bar^{-1} and rejection of 91% after a 40 h separation process in DMSO. This study not only provides a useful reference for the preparation of high-performance solvent-resistant nanofiltration membrane materials using polyphenols as raw materials, but also provides ideas for reducing energy consumption, material consumption, and carbon emission.

Supplementary Materials

Table S1: lists the swelling degree of NF-1OL-2U in THF, Methanol, DMF, DMSO, and NMP.

Figure S1: lists the effects of microwave time on membrane properties.

Author Contributions

Ayang Zhou: Conceptualization, Writing, Supervision. Mengying Li: Software, Formal analysis. Lin Li: Methodology, Yujie, Wang.: Resources & Editing.

Data Availability

The data supporting the findings of this study are available within the manuscript and the supplementary materials.

Conflicts of Interest

All authors declare that there are no conflicts of interest or personal relationships that could have appeared to influence this paper.

Funding

This work was supported by the University Natural Science Research Key Project of Anhui Province, (KJ2020A0707). Key Projects of the Excellent Young Talents Support Plan in Universities of Anhui Province (gxyq2021218). University Natural Science Research Major Project of Anhui Province, (KJ2019ZD043).

References

[1] Wang X, Wang N, Li X, An Q-F. A review of nano-confined composite membranes fabricated inside the porous support. Advanced Membranes 2021;1:100005. https://doi.org/10.1016/j.advmem.2021.100005.

[2] Zhu J, Yuan S, Wang J, Zhang Y, Tian M, Van der Bruggen B. Microporous organic polymer-based membranes for ultrafast molecular separations. Progress in Polymer Science 2020;110:101308. https://doi.org/10.1016/j.progpolymsci.2020.101308.

[3] Mohammad AW, Teow YH, Ang WL, Chung YT, Oatley-Radcliffe DL, Hilal N. Nanofiltration membranes review: Recent

advances and future prospects. Desalination 2015;356:226–54. https://doi.org/10.1016/j.desal.2014.10.043.

[4] Almijbilee MMA, Wu X, Zhou A, Zheng X, Cao X, Li W. Polyetheramide organic solvent nanofiltration membrane prepared via an interfacial assembly and polymerization procedure. Separation and Purification Technology 2020;234:116033. https://doi.org/10.1016/j.seppur.2019.116033.

[5] Shi GM, Feng Y, Li B, Tham HM, Lai J-Y, Chung T-S. Recent progress of organic solvent nanofiltration membranes. Progress in Polymer Science 2021;123:101470. https://doi.org/10.1016/j.progpolymsci.2021.101470.

[6] Ignacz G, Yang C, Szekely G. Diversity matters: Widening the chemical space in organic solvent nanofiltration. Journal of Membrane Science 2022;641:119929. https://doi.org/10.1016/j.memsci.2021.119929.

[7] Scharzec B, Holtkötter J, Bianga J, Dreimann JM, Vogt D, Skiborowski M. Conceptual study of co-product separation from catalyst-rich recycle streams in thermomorphic multiphase systems by OSN. Chemical Engineering Research and Design 2020;157:65–76. https://doi.org/10.1016/j.cherd.2020.02.028.

[8] Zhao Y, Tong T, Wang X, Lin S, Reid EM, Chen Y. Differentiating Solutes with Precise Nanofiltration for Next Generation Environmental Separations: A Review. Environ Sci Technol 2021;55:1359–76. https://doi.org/10.1021/acs.est.0c04593.

[9] Emami MRS, Amiri MK, Zaferani SPG. Removal efficiency optimization of Pb2+ in a nanofiltration process by MLP-ANN and RSM. Korean J Chem Eng 2021;38:316–25. https://doi.org/10.1007/s11814-020-0698-8.

[10] Zhang Y, Song Q, Liang X, Wang J, Jiang Y, Liu J. High-flux, high-selectivity loose nanofiltration membrane mixed with zwitterionic functionalized silica for dye/salt separation. Applied Surface Science 2020;515:146005. https://doi.org/10.1016/j.apsusc.2020.146005.

[11] Gohain MB, Pawar RR, Karki S, Hazarika A, Hazarika S, Ingole PG. Development of thin film nanocomposite membrane incorporated with mesoporous synthetic hectorite and MSH@UiO-66-NH2 nanoparticles for efficient targeted feeds separation, and antibacterial performance. Journal of Membrane Science 2020;609:118212. https://doi.org/10.1016/j.memsci.2020.118212.

[12] He X, Zhou A, Shi C, Zhang J, Li W. Solvent resistant nanofiltration membranes using EDA-XDA co-crosslinked poly(ether imide). Separation and Purification Technology 2018;206:247–55. https://doi.org/10.1016/j.seppur.2018.05.031.

[13] Wang C, Zhang J, Liu C, Song X, Zhang C. Wood–inspired preparation of ligninsulfonate/trimesoylchloride nanofilm with a highly negatively charged surface for removing anionic dyes. Chemical Engineering Journal 2021;412:128609. https://doi.org/10.1016/j.cej.2021.128609.

[14] Wang C, Zhang J, Song X, Zhang C. Ligninsulfonate/trimesoylchloride nanocomposite membrane with transmembrane nanochannels via bionic cell membrane for molecular separation. Journal of Membrane Science 2021;638:119741. https://doi.org/10.1016/j.memsci.2021.119741.

[15] Jimenez-Solomon MF, Song Q, Jelfs KE, Munoz-Ibanez M, Livingston AG. Polymer nanofilms with enhanced microporosity by interfacial polymerization. Nature Mater 2016;15:760–7. https://doi.org/10.1038/nmat4638.

[16] Abdellah MH, Pérez-Manríquez L, Puspasari T, Scholes CA, Kentish SE, Peinemann K-V. A catechin/cellulose composite membrane for organic solvent nanofiltration. Journal of Membrane Science 2018;567:139–45. https://doi.org/10.1016/j.memsci.2018.09.042.

[17] Zhu C-Y, Liu C, Yang J, Guo B-B, Li H-N, Xu Z-K. Polyamide nanofilms with linearly-tunable thickness for high performance nanofiltration. Journal of Membrane Science 2021;627:119142. https://doi.org/10.1016/j.memsci.2021.119142.

[18] Zhai Z, Jiang C, Zhao N, Dong W, Li P, Sun H, *et al*. Polyarylate membrane constructed from porous organic cage for high-performance organic solvent nanofiltration. Journal of Membrane Science 2020;595:117505. https://doi.org/10.1016/j.memsci.2019.117505.

[19] Karki S, Gohain MB, Yadav D, Ingole PG. Nanocomposite and bio-nanocomposite polymeric materials/membranes development in energy and medical sector: A review. International Journal of Biological Macromolecules 2021;193:2121–39. https://doi.org/10.1016/j.ijbiomac.2021.11.044.

[20] Karki S, Ingole PG. Chapter Four - Graphene-based thin film nanocomposite membranes for separation and purification. In: Hussain CM, editor. Comprehensive Analytical Chemistry, vol. 91, Elsevier; 2020, p. 73–97. https://doi.org/10.1016/bs.coac.2020.08.005.

[21] Pouteau C, Dole P, Cathala B, Averous L, Boquillon N. Antioxidant properties of lignin in polypropylene. Polymer Degradation and Stability 2003;81:9–18. https://doi.org/10.1016/S0141-3910(03)00057-0.

[22] Qin J, Woloctt M, Zhang J. Use of Polycarboxylic Acid Derived from Partially Depolymerized Lignin As a Curing Agent for Epoxy Application. ACS Sustainable Chem Eng 2014;2:188–93. https://doi.org/10.1021/sc400227v.

[23] Gosselink RJA, Abächerli A, Semke H, Malherbe R, Käuper P, Nadif A, *et al*. Analytical protocols for characterisation of sulphur-free lignin. Industrial Crops and Products 2004;19:271–81. https://doi.org/10.1016/j.indcrop.2003.10.008.

[24] Zhou A, Almijbilee MMA, Zheng J, Wang L. A thin film composite membrane prepared from monomers of vanillin and trimesoyl chloride for organic solvent nanofiltration. Separation and Purification Technology 2021;263:118394. https://doi.org/10.1016/j.seppur.2021.118394.

[25] Zhou A, Shi C, He X, Fu Y, Anjum AW, Zhang J, *et al*. Polyarylester nanofiltration membrane prepared from monomers of vanillic alcohol and trimesoyl chloride. Separation and Purification Technology 2018;193:58–68. https://doi.org/10.1016/j.seppur.2017.10.047.

[26] Zhou A, Wang Y, Cheng D, Li M, Wang L. Effective interfacially polymerized polyarylester solvent resistant nanofiltration membrane from liquefied walnut shell. Korean J Chem Eng 2022;39:1566–75. https://doi.org/10.1007/s11814-021-1048-1.

[27] Zhou A, Wang Y, Almijbilee MMA, Wang Y, Cheng D. A thin-film composite polyarylester membrane prepared from orcinol and trimesoyl chloride for organic solvent nanofiltration. Iran Polym J 2022;31:1021–32. https://doi.org/10.1007/s13726-022-01054-8.

[28] Li W, Bian C, Fu C, Zhou A, Shi C, Zhang J. A poly(amide-co-ester) nanofiltration membrane using monomers of glucose and

trimesoyl chloride. Journal of Membrane Science 2016;504:185–95. https://doi.org/10.1016/j.memsci.2015.12.064.

[29] Zhou A, Li L, Li M, Chen Q. Fabrication of Poly(amide-co-ester) Solvent Resistant Nanofiltration Membrane from P-nitrophenol and Trimethyl Chloride via Interfacial Polymerization. Separations 2022;9:28. https://doi.org/10.3390/separations9020028.

[30] Van der Bruggen B, Jansen JC, Figoli A, Geens J, Van Baelen D, Drioli E, *et al*. Determination of Parameters Affecting Transport in Polymeric Membranes: Parallels between Pervaporation and Nanofiltration. J Phys Chem B 2004;108:13273–9. https://doi.org/10.1021/jp048249g.

[31] Jimenez Solomon MF, Bhole Y, Livingston AG. High flux membranes for organic solvent nanofiltration (OSN)—Interfacial polymerization with solvent activation. Journal of Membrane Science 2012;423–424:371–82. https://doi.org/10.1016/j.memsci.2012.08.030.

[32] Albrecht W, Seifert B, Weigel T, Schossig M, Holländer A, Groth T, *et al*. Amination of Poly(ether imide) Membranes Using Di- and Multivalent Amines. Macromolecular Chemistry and Physics 2003;204:510–21. https://doi.org/10.1002/macp.200390016.

[33] Roy S, Yue CY, Venkatraman SS, Ma LL. Low-temperature (below Tg) thermal bonding of COC microfluidic devices using UV photografted HEMA-modified substrates: high strength, stable hydrophilic, biocompatible surfaces. J Mater Chem 2011;21:15031–40. https://doi.org/10.1039/C1JM11750E.

[34] Zhang R, Yu S, Shi W, Wang W, Wang X, Zhang Z, *et al*. A novel polyesteramide thin film composite nanofiltration membrane prepared by interfacial polymerization of serinol and trimesoyl chloride (TMC) catalyzed by 4-dimethylaminopyridine (DMAP). Journal of Membrane Science 2017;542:68–80. https://doi.org/10.1016/j.memsci.2017.07.054.

[35] Li Y, Xue J, Zhang X, Cao B, Li P. Formation of Macrovoid-Free PMDA-MDA Polyimide Membranes Using a Gelation/Non-Solvent-Induced Phase Separation Method for Organic Solvent Nanofiltration. Ind Eng Chem Res 2019;58:6712–20. https://doi.org/10.1021/acs.iecr.9b00623.

[36] Xing DY, Chan SY, Chung T-S. The ionic liquid [EMIM]OAc as a solvent to fabricate stable polybenzimidazole membranes for organic solvent nanofiltration. Green Chem 2014;16:1383–92. https://doi.org/10.1039/C3GC41634H.

[37] Aburabie J, Emwas A-H, Peinemann K-V. Silane-Crosslinked Asymmetric Polythiosemicarbazide Membranes for Organic Solvent Nanofiltration. Macromolecular Materials and Engineering 2019;304:1800551. https://doi.org/10.1002/mame.201800551.

[38] Aburabie J, Neelakanda P, Karunakaran M, Peinemann K-V. Thin-film composite crosslinked polythiosemicarbazide membranes for organic solvent nanofiltration (OSN). Reactive and Functional Polymers 2015;86:225–32. https://doi.org/10.1016/j.reactfunctpolym.2014.09.011.

[39] Sun S-P, Chung T-S, Lu K-J, Chan S-Y. Enhancement of flux and solvent stability of Matrimid® thin-film composite membranes for organic solvent nanofiltration. AIChE Journal 2014;60:3623–33. https://doi.org/10.1002/aic.14558.

[40] Lu T-D, Chen B-Z, Wang J, Jia T-Z, Cao X-L, Wang Y, *et al*. Electrospun nanofiber substrates that enhance polar solvent separation from organic compounds in thin-film composites. J Mater Chem A 2018;6:15047–56. https://doi.org/10.1039/C8TA04504F.

How to Cite

Zhou A, Li M, Li L, Wang Y. Preparation and Performance Control of Orcinol Composite Nanofiltration Membrane for Dimethyl Sulfoxide Recovery. Membrane Sci Int 2022;1(2):44–53.